Journal of Cerebral Blood Flow & Metabolism (2012) 32, 2055–2065

www.jcbfm.com

A novel population of α-smooth muscle actin-positive cells activated in a rat model of stroke: an analysis of the spatio-temporal distribution in response to ischemia

Varun Sharma[1,6], Tina W Ling[1,6], Sarah S Rewell[2,3], David L Hare[1,2], David W Howells[4], Angela Kourakis[2] and Peter J Wookey[2,5]

[1]*Cardiology Department, Austin Health, Melbourne, Victoria, Australia;* [2]*Department of Medicine, University of Melbourne, Austin Health, Melbourne, Victoria, Australia;* [3]*Florey Neuroscience Institutes, Melbourne, Victoria, Australia;* [4]*National Stroke Research Institute, Melbourne, Victoria, Australia;* [5]*Centre for Neuroscience, University of Melbourne, Melbourne, Victoria, Australia*

In a rat model of stroke, the spatio-temporal distribution of α-smooth muscle actin-positive, (αSMA+) cells was investigated in the infarcted hemisphere (ipsilateral) and compared with the contralateral hemisphere. At day 3 postischemia, αSMA+ cells were concentrated in two main loci within the ipsilateral hemisphere (Area A) in the medial corpus callosum and (Area B) midway through the striatum adjacent to the lateral ventricle. By day 7 and further by day 14, fewer αSMA+ cells remained in Areas A and B but a steady increase in the peri-infarct was observed. αSMA+ cells also expressed glial acidic fibrillary protein [GFAP: αSMA+/GFAP+ (29%); αSMA+/GFAP− (71%) phenotypes] and feline leukemia virus C receptor 2 (FLVCR2), but not ED1(microglia) and established markers of pericytes normally located in vascular wall. αSMA+ cells were also located close to the subventricular zones (SVZ) adjacent to Areas A and B. In conclusion, αSMA+ cells have been identified in a spatial and temporal sequence from the SVZ, at intermediate loci and in the vicinity of the peri-infarct. It is hypothesized that novel populations of αSMA+ precursors of pericytes are born on the SVZ, migrate into the peri-infarct region and are incorporated into new vessels of the peri-infarct regions.
Journal of Cerebral Blood Flow & Metabolism (2012) **32,** 2055–2065; doi:10.1038/jcbfm.2012.107; published online 18 July 2012

Keywords: acute stroke; animals models; brain ischemia; pericytes; vascular biology

Introduction

In stroke, complex molecular, cellular, and inflammatory mechanisms are activated in response to the induction of ischemia, and many cells adapt to the hypoxic conditions of the damaged tissue and periphery (peri-infarct) to initiate restoration of compromised neuronal networks. Underlying this restoration is a set of responses aimed at the reestablishment of an ordered blood supply.

Migration of immature cell types from sites of proliferation towards damaged brain tissue is an important feature for the restriction of damage, the stabilization of tissues and surviving cells in the regions surrounding the lesion, and the restoration of function. Several studies have investigated the increase in precursor migrations from the subventricular zones (SVZ) after trauma in the cerebral cortex (Jin *et al*, 2001; Zhang *et al*, 2001; Parent *et al*, 2002; Goings *et al*, 2004). In adult mice, cortical lesions induced the birth and migration of new glial cells, some of which pass into the corpus callosum where they survived for at least 3 weeks (Goings *et al*, 2004). In adult rats, in which labeling of early proliferating cells such as glia was avoided in response to focal ischemia, there was a general increase in neuroblast migration from the SVZ along the rostral migratory stream but some cells were directed towards the site of lesion (Parent *et al*, 2002). An important component of the SVZ is the vascular niche for

Correspondence: Dr PJ Wookey, Department of Medicine, University of Melbourne, Lance Townsend Building, Level 10, Austin Campus, Austin Health, Studley Road, Heidelberg VIC 3084, Australia.
E-mail: pwookey@unimelb.edu.au
[6]These authors contributed equally to this work.
Received 17 April 2012; revised 20 June 2012; accepted 21 June 2012; published online 18 July 2012

neural stem/progenitor cells (NSPCs) (Tavazoie *et al*, 2008) from which SVZ-derived NSPCs migrate into the striatum along blood vessels in response to ischemia (Kojima *et al*, 2010). In mild cortical strokes, NSPCs do not appear to migrate from the SVZ but arise locally (Shimada *et al*, 2010). Furthermore, alternative sites of proliferation of NSPCs have been defined in the neocortical layer (Ohira *et al*, 2010) and pia mater (Nakagomi *et al*, 2011).

Particular cell types also infiltrate the ischemic core and rim, including nestin+ progenitors (Kronenberg *et al*, 2005; Nakagomi *et al*, 2009) and bone marrow-derived progenitor cells of pericytes. Pericytes and endothelial precursors are two important cell types that contribute directly to the reestablishment of the vasculature in the peri-infarct regions and become activated in response to ischemia, as described in numerous studies (Jeynes, 1985; Takahashi *et al*, 1997; Renner *et al*, 2003; Yemisci *et al*, 2009).

Two reports attribute adult bone marrow as the source of precursor cells of pericytes that are recruited into blood vessels during angiogenesis in the peri-infarct regions of damaged tissues following the induction of stroke (Kokovay *et al*, 2006; Lamagna and Bergers, 2006). In the study by Kokovay *et al* (2006), pericytes were identified as being derived from bone marrow, desmin-positive and bounded by laminin layers (basement membrane) that surround new blood vessels of the infarct region of the striatum. However, in view of the disparate origins of the cellular components of the vascular wall during angiogenesis (Pardanaud *et al*, 1989) in developing brain (including pericytes (Etchevers *et al*, 2001)), which depends on the anatomical location of blood vessels in question, it raises the possibility that the sources of pericytes recruited into damaged tissue resulting from stroke might depend on the site of lesion, and available access routes to the periphery of ischemic tissue. In this regard in the developing fetal brain, the dorso-posterior vascular compartment, including pericytes, originates from cephalic paraxial mesoderm, but the cellular components of ventro-anterior vessels are derived entirely from NCCs (neural crest cells) (Etchevers *et al*, 2001) that migrate from the site of proliferation. Thus, infarcts in different regions of the brain and different destinations within the peri-infarct might require recruitment of pericytes from separate sources.

Pericyte precursors have been found to be multipotential (Dore-Duffy *et al*, 2011) and furthermore, immortalized multipotential precursors were α-smooth muscle actin (αSMA)-negative *in vitro* (Dore-Duffy, 2008; Dore-Duffy *et al*, 2011). However, transforming growth factorβ has been reported to induce αSMA in the brain (Verbeek *et al*, 1994) and retinal (Sieczkiewicz and Herman, 2003) pericytes, perhaps suggesting that αSMA-expression (αSMA+) can be associated with a more mature phenotype. The possibility that pericytes might express the feline leukemia virus C receptor 2 (FLVCR2) transporter (Brasier *et al*, 2004) of heme (Duffy *et al*, 2010) as described during angiogenesis in fetal development of the brain (Thomas *et al*, 2010) warranted an investigation of its expression in the adult brain by the αSMA+ cells described in this study.

In this study, a population of αSMA+ cells with a unique morphology is described together with the spatio-temporal distribution of concentrations of these cells, activated following the temporary occlusion of the middle cerebral artery (MCAO) in a rat model of stroke. Thus, the time-dependent changes in concentrations of αSMA+ cells at specific loci on the ipsilateral, ischemic hemisphere were compared at several time points after MCAO, but these were not found in the contralateral control hemisphere.

Materials and methods

Preparation of the Spontaneously Hypertensive Rat Model of Stroke

The thread occlusion model of MCAO was used to induce stroke in 15-week-old male spontaneously hypertensive rats (SHR) (Animal Research Centre, Perth, WA, Australia). Anesthesia was induced using 5% Isoflurane (50:50 for oxygen: air mix) and maintained at 2% in freely breathing animals via a nose cone. To induce infarction, a 90-minute transient MCAO using a thread occlusion was performed as previously described (Rewell *et al*, 2010) with modifications recommended earlier by Spratt *et al* (2006). In brief, the suture (silicone-coated, with a diameter of 0.35 mm and length 2 mm) was inserted through the right external carotid and up through the internal carotid artery to occlude the right MCA. Laser Doppler flowmetry was used to detect a drop in cerebral blood flow, which was the criterion used for successful occlusion. Rectal temperature was maintained at 37.4°C (temperature control units were manufactured 'in house' and consisted of a thermocouple connected to a heat mat, which is regulated by the temperature control box). Blood oxygen levels and heart rate were monitored. After 90 minutes, the animals were anaesthetized once again and the suture obstructing the MCA was removed. Animals were randomized to each experimental group (time of survival). The assessment of neurological symptoms was performed at 1.5 and 24 hours postocclusion according to a slightly modified procedure outlined by Petullo *et al* (1999), with the investigator blinded to experimental group. At several time points post-MCAO (day 1, day 3, day 7, and day 14), the animals were euthanized and perfused with 0.9% saline followed by 4% paraformaldehyde (pfa)/phosphate-buffered saline (PBS). All procedures were carried out in accordance with institutional (Animal Ethics Committee of Austin Health, approval number 2007-2796) and national (National Health and Medical Research Council and ARRIVE) guidelines.

Initially, three rats were used for each time point (days 1, 3, 7, 14), with four sections from each rat being stained for αSMA. Variable numbers of αSMA+ cells were initially observed at days 3, 7, and 14 poststroke in most animals, and therefore the sample size was increased from 3 rats to 11 rats for each of these time points to achieve statistical significance. Thus, four sections were counted from 11 animals making a total of 44 sections per time point.

Paraffin Embedded Sections

The brains were removed from the skulls and postfixed for 24 hours in 4% pfa/PBS. Tissue was then cut into 2 mm thick coronal slices using a rat brain matrix. Slices were embedded in paraffin using standard histological techniques. Paraffin embedded sections were cut at a thickness of 7 μm using a microtome (Leica, Solms, Germany). Sections were collected on to silane (3-aminopropyltriethoxysilane [APES]; Sigma-Aldrich, St Louis, MO, USA) coated slides in series of 20 each, with the 1st, 21st, 41st, and 61st sections mounted on slide 1, resulting in a distance of $\sim$140 μm between each section on a slide. Four tissue sections (1 slide) from each rat were stained for αSMA.

Immunohistochemistry

An amplified tyramide-based protocol was used for immunohistochemistry (CSA II kit, DAKO, Glostrup, Denmark). The anti-human/rat αSMA antibody (mouse monoclonal clone 1A4, M0851, DAKO, identical to αsm-1 (Skalli *et al*, 1986)) was provided as 70 μg/mL and diluted 1:500. Sections were then counter-stained with hematoxylin (Amber Scientific, Midvale, WA, Australia).

Images of tissue sections (TIF files) were captured with an Olympus (Tokyo, Japan) BX50 microscope, mounted with a Leica DFC 490 digital camera, and the Leica Application Suite 2.8.1. Areas of αSMA staining (Figures 1B and 1C) were identified and images (examples Figures 1D and 1E) captured for analysis using the MCID image analysis suite (insert Figure 1B, MCID Analysis 7.0, Rev 2.0, InterFocus Imaging, Cambridge, UK). A set of hue, intensity, and saturation settings were fixed to identify αSMA densities. The number of αSMA-positive entities was quantified using the automated quantification mode of MCID in which the field size and stain count area were kept constant for all quantification. These data were transferred to MS Excel (Microsoft® Office Excel, 2007) for data analysis and statistical interpretation. Inbuilt functions on MS Excel were used to calculate standard deviation, standard errors, count averages, and independent one-sample *t*-tests.

Preparation of Frozen Sections

The time points post-MCAO investigated in this part of the study included days 1, 3, 7, and 14. The perfused brains were removed from the skull, washed in PBS, and stored in PBS-sucrose-azide solution (PBS containing 30% sucrose and 0.1% sodium azide) as a cryoprotectant at 4°C for 24 hours before being snap frozen in isopentane/dry ice. Frozen brains were stored at −80°C before being sectioned at 20 μm on a cryostat (Microm HM505E) and collected on Superfrost Plus slides (Menzel-Glaser, Braunschweig, Germany).

Immunofluorescence

Immunohistochemistry using an immunofluorescence protocol was performed with antibodies against αSMA (1:200 dilution, mouse IgG2A DAKO M0851), PDGFRβ (platelet-derived growth factor receptor-β; 1:100, rabbit polyclonal Santa Cruz SC432, Santa Cruz, CA, USA), Ki67 (1:50 to 100, rabbit polyclonal Millipore AB9260, Billerica, MA, USA), NG2 (1:100, mouse IgG1 Millipore MAB5384), FLVCR2 (1:50 of 1 mg/mL, mouse IgG1 Mab 3D5 [made by Dr Wookey] and 1:50 of 1 mg/mL, mouse IgG3, MAb 33/01-4A5 [made by Dr Wookey], also known as MCA2322, AbD-Serotec, Oxford, UK), nestin (1:200, mouse IgG1 R&D Systems MAB1259, Minneapolis, MN, USA) and desmin (1:50, rabbit polyclonal, Millipore AB907). GFAP (glial fibrillary acidic protein) was used to identify astrocytes (1:500 chicken polyclonal, Millipore AB5541) and the mouse monoclonal ED1 (IgG1, 1:100, AbD-Serotec, MCA341R) to identify CD68 expressed by rat microglia and macrophages. Appropriate secondary antibodies [goat anti-mouse isotypes IgG1, IgG2A, IgG3, goat anti-rabbit and goat anti-chicken conjugated to AlexaFluors (488, 568, and 633 nm), Invitrogen, Carlsbad, CA, USA] at 1:500 dilutions were used to develop fluorescence.

Slides with frozen rat brain sections were left to dry at room temperature for approximately an hour before being postfixed in 4% pfa/PBS for 1 hour. Sections were washed twice for 5 minutes in PBS/1% Triton X-100 (pH 7.4) before being blocked with 5% normal goat serum in PBS/1% Triton X-100 (block solution) for 1 hour at room temperature. The sections were then covered with primary antibodies (diluted in block solution as indicated above) and incubated overnight at 6°C in a humidified chamber. The next day, sections were washed in PBS/1% Triton X-100 for 3×10 minutes in a coplin jar, while being agitated gently on a rotator table. Secondary antibodies were then layered onto sections (at dilutions indicated above in PBS), with incubation for 90 minutes at room temperature in the dark to prevent bleaching of fluorescence. Sections were washed again in PBS for 3×10 minutes while being agitated gently on a rotator table. Prolong Gold mountant (Invitrogen, containing the DAPI nuclear stain; 4′,6-diamidino-2-phenylindole) was then applied on coverslips and left to dry for 2 days in the dark before imaging with the confocal microscope.

Confocal Microscopy

Tissues were examined using a Zeiss Meta confocal laser scanning system incorporating Zen software (Zeiss, Oberkochen, Germany). A 405-nm excitation filter was used to visualize DAPI (nuclear staining), and a 488-nm excitation filter was used for Alexa 488 secondary antibody. A 561-nm excitation filter and 633-nm excitation filter were used to visualize Alexa 568 and 633 secondary antibodies, respectively. Images were captured in a single focal plane with optical sections of 0.5 μm nominal thickness or using deconvolution of *Z*-plane stacks to generate compressed single plane images of up to 20 μm tissue thickness.

Results

The Locations of Areas of High Density of α-Smooth Muscle Actin + Cells Within the Ipsilateral Hemisphere

Area A is located medially in the corpus callosum on the dorsal horn of the lateral ventricle, adjacent to

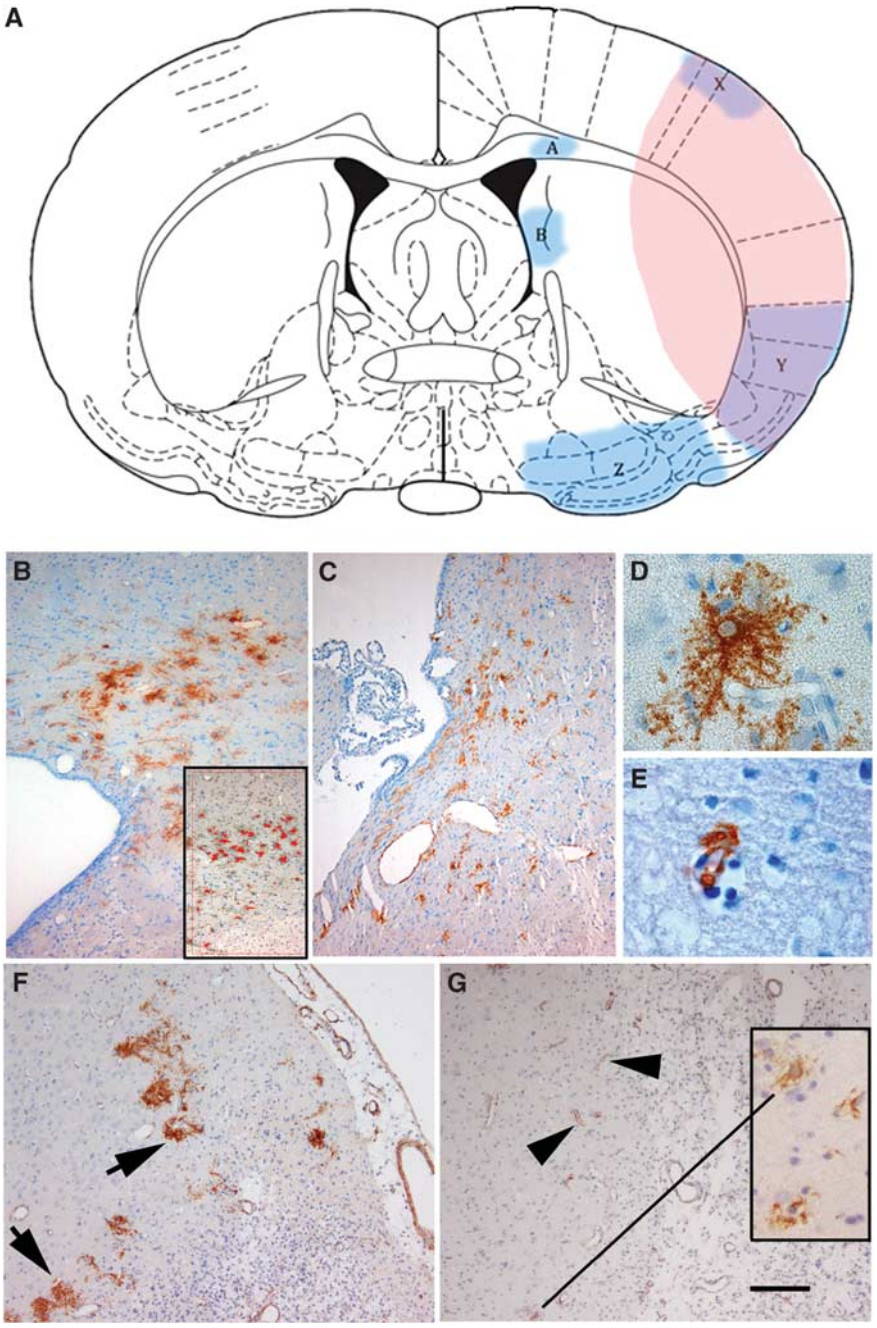

Figure 1 (**A**) A schematic of a coronal section of rat brain following occlusion of the middle cerebral artery (MCAO). The areas of pink/purple represent the extent of a typical area of infarct including areas of cerebral cortex and striatum. Areas A (**B**, day 3), B (**C**, day 3), X, Y, and Z are indicated as regions of considerable concentrations of αSMA + cells. The insert in (**B**) shows the highlighting in red generated by the MCID program to identify intense staining and count these αSMA + ve cells. (**D** (Morphology 1), **E** (Morphology 2)) Representative αSMA + cells identifiable with light microscopy. (**F**) (day 7, Area X) αSMA + cells (arrowed, predominantly Morphology 1) aligned around the infarct area (indicated with dense populations of nucleated cells). By day 14 in Area X, relatively few αSMA + cells display Morphology 1 and the majority of staining is associated with small vessels (Morphology 2, arrowheads and insert in (**G**)). The calibration bar in (**G**) represents 1.1 mm in (**A**), 100 μm in (**B**, **C**, **F**, **G**), and 25 μm in (**D**, **E**). SMA, smooth muscle actin.

the junction of the caudate putamen while Area B is located further ventrally approximately midway through the medial edge of the caudate putamen, adjacent to the lateral ventricle (Figure 1A). Area X covers the dorso-lateral aspects of the parietal cortex while Area Y covers the ventral aspects of the parietal cortex, extending into the dorsal aspects of the insular cortex and the ventro-lateral apex of the

caudate putamen. Areas X and Y are both in the lateral borders of the region of infarct, suggesting a location in the penumbra of the infarct.

Areas A and B are both adjacent to SVZ of proliferation on the lateral ventricles as indicated in coronal section (Figure 1A). The peri-ventricular nature of Area Z is not evident in the coronal schematic shown in Figure 1A, but in a sagittal section (not shown) Area Z is immediately anterior to the inferior horn of the lateral ventricle.

Morphology of α-Smooth Muscle Actin + Cells

Under low power light microscopy, two distinct morphologies of αSMA + cells were evident in Areas A and B at day 3 (Figures 1B and 1C). The predominant morphology here, an example of which is shown in panel D, bears multiple cytoplasmic projections and has a pale nucleus [Morphology 1]. A high proportion (>90%) of αSMA + cells in peri-SVZ areas (Areas A and B, day 3) and Area X (day 7) displayed this morphology.

There was also a small proportion of αSMA + cell in Area A (day 3) associated with blood vessels [Morphology 2] (Figure 1E). Morphology 2 was the predominant form of αSMA + cells present in the regions of infarct (Areas X and Y) at day 14 (Figure 1G and insert), although <10% of the αSMA + cells at day 7 (Area X) displayed Morphology 2 (Figure 1F).

Quantification of α-Smooth Muscle Actin + Cells in Areas A, B, X, Y, and Z

At day 1 post-infarct, very few αSMA + cells could be identified in either ipsilateral or contralateral tissues with the exception of αSMA + cells surrounding some large blood vessels. By day 3, large numbers of αSMA + cells were found at specific loci on the ipsilateral side but few positive cells were evident on the contralateral hemisphere (Figures 3C and 3F), which served as a negative control.

At day 3 post-infarct, αSMA + cells were concentrated in Area A (corpus callosum, Figures 1A and 1B; examples at high magnification, Figures 1D and 1E). Similarly, densities of αSMA + cells were located in Area B (Figure 1C) at day 3. At this time point, few cells expressed αSMA + in the peri-infarct equivalent to Areas X, Y, or Z (data not shown).

By day 7, fewer cells were counted in Area A and the difference between days 3 and 7 was statistically significant (Figure 2, $P=0.015$). In Areas B and Z, although there appeared to be increased numbers of cells (day 7 compared with day 3), there was no statistically significant difference. By contrast in the peri-infarct Areas X and Y, there were increases (day 7 compared with day 3) in the densities of cells expressing αSMA that were statistically significant ($P=0.0001$).

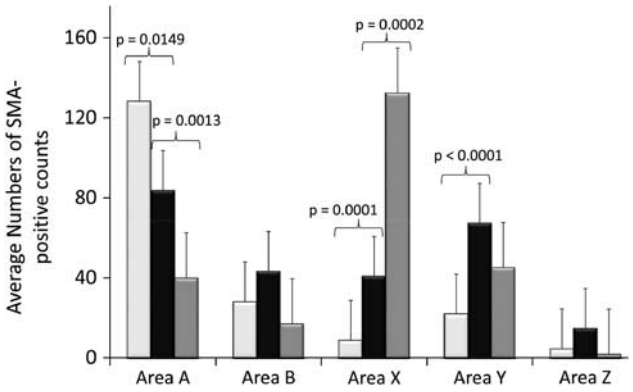

Figure 2 Histogram representing the quantification of αSMA + cell numbers. The averages per section at day 3 (▒), day 7 (■), and day 14(■) post-infarct are shown for Areas A, B, X, Y, and Z. At days 3 and 7, the counts represent >90% Morphology 1, while at day 14 (Area X), most counts (>90%) represent Morphology 2. SMA, smooth muscle actin.

By day 14 (Figure 2), the numbers of αSMA + cells counted in Area A had dropped to 30% of the value for day 3 and there were fewer than found in day 7, which was statistically significant ($P=0.0013$). The counts in Area X at this time represent few αSMA + cells with Morphology 1 (<10%) while most staining was associated with an increased number of αSMA + vessels (Morphology 2, Figure 1G).

In contrast, there was no change in Area B detected as statistically significant in the numbers of αSMA + cells from days 3 to 14.

Other Markers Expressed by α-Smooth Muscle Actin + Cells

Confocal microscopy was used with multilabeling techniques and *Z*-plane deconvolution to explore other markers that might be expressed by αSMA + cells with Morphology 1.

At day 3 (Figure 3), relatively high numbers of αSMA + cells were located in Areas A and B (Figures 1 and 2) and therefore these Areas were investigated for evidence of coexpression of other markers with αSMA. Evidence of coexpression of GFAP with αSMA (Figures 3A and 3D) was found in 29% of αSMA + cells [71% αSMA + cells were GFAP−] in these Areas at day 3 (Figures 3B and 3E). In contrast, there were few αSMA + cells found in equivalent regions of the contralateral hemisphere (Figures 3C and 3F).

The coexpression of αSMA + /GFAP + (Lecain *et al*, 1991) is consistent with expression by subpopulations of multipotential precursors of pericytes cultured *in vitro* (Dore-Duffy *et al*, 2011). For this reason, other markers of precursors (nestin) and pericytes were investigated and these included desmin (Kokovay *et al*, 2006), NG2 (Kokovay *et al*, 2006; Dore-Duffy *et al*, 2011), PDGFRβ (Lindahl *et al*, 1997; Dore-Duffy *et al*, 2011) and FLVCR2 (Thomas *et al*, 2010). At day 3 in Areas A and B,

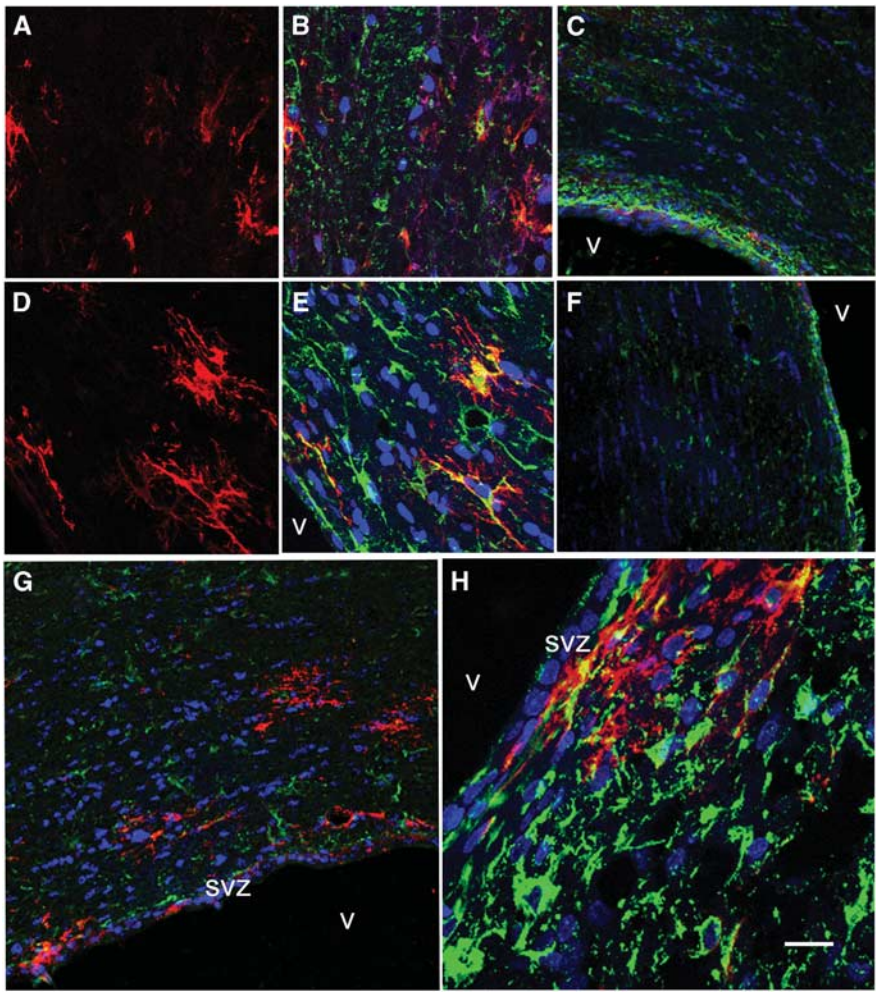

Figure 3 (**A**) At day 3, αSMA + cells (red) in Area A. (**B**) The same field as a color composite (αSMA, red; glial fibrillary acidic protein (GFAP), green; NG2, pink; DAPI, blue) in which there are examples of αSMA + /GFAP + cells (yellow). (**C**) A region equivalent to Area A at low magnification, but on the contralateral hemisphere. (**D**) αSMA + cells (red) in Area B. (**E**) Same field as a color composite (αSMA, red; GFAP, green; NG2, pink; DAPI, blue) in which there are examples of αSMA + /GFAP + cells (yellow). (**F**) A region equivalent to Area B at low magnification, but on the contralateral side. (**G**, **H**) Two regions adjacent to the subventricular zones (SVZ) are shown as composites (αSMA, red; GFAP, green; DAPI, blue): (G) a region close to Area A and (**H**) close to Area B. The lateral ventricle is indicated with V and the subventricular zones with SVZ. The calibration bar in (**H**) represents 40 μm in (**A**, **B**, **D**, **E**), 100 μm in (**C**, **F**), and 50 μm in (**G**, **H**). SMA, smooth muscle actin.

there was no obvious costaining of αSMA with desmin, NG2, PDGFRβ or FLVCR2. In the adjacent SVZ (Figures 3G and 3H), αSMA + cells were negative for nestin.

At day 7, numbers of αSMA + cells (Morphology 1) had increased in the peri-infarct regions of Areas X, Y, and Z (Figures 1 and 2). Once again there was no evidence of coexpression of these pericyte markers with these αSMA + cells (Morphology 1) although cells in Areas A (Figures 4L–N) and X (Figures 4O–Q) expressed FLVCR2 (detected with MAb 3D5) and these were GFAP + (not shown). FLVCR2 expression (detected with MAb 3D5, raised against an extracellular epitope) was confirmed using MAb 33/01-4A5 raised against an intracellular epitope of FLVCR2 (data not shown).

Colocalization of α-Smooth Muscle Actin and ED1, a Marker of Microglia and Macrophages

At day 7, populations of cells that stained positive for the marker ED1 (CD68), namely rat microglia and macrophages, were investigated at key loci, some of which are illustrated in Figure 4. Large numbers of ED1-positive cells were evident in the damaged infarct tissue (above white line in Figure 4A), whereas there were fewer in the adjacent peri-infarct (Area X, below white line). Fewer ED1-positive cells were evident in Area A (Figure 4B) and these could be clearly distinguished from αSMA + cells with Morphology 1 and GFAP + cells (data not shown). One prominent ED1 cell was found protruding into the ventricular space (Figure 4B).

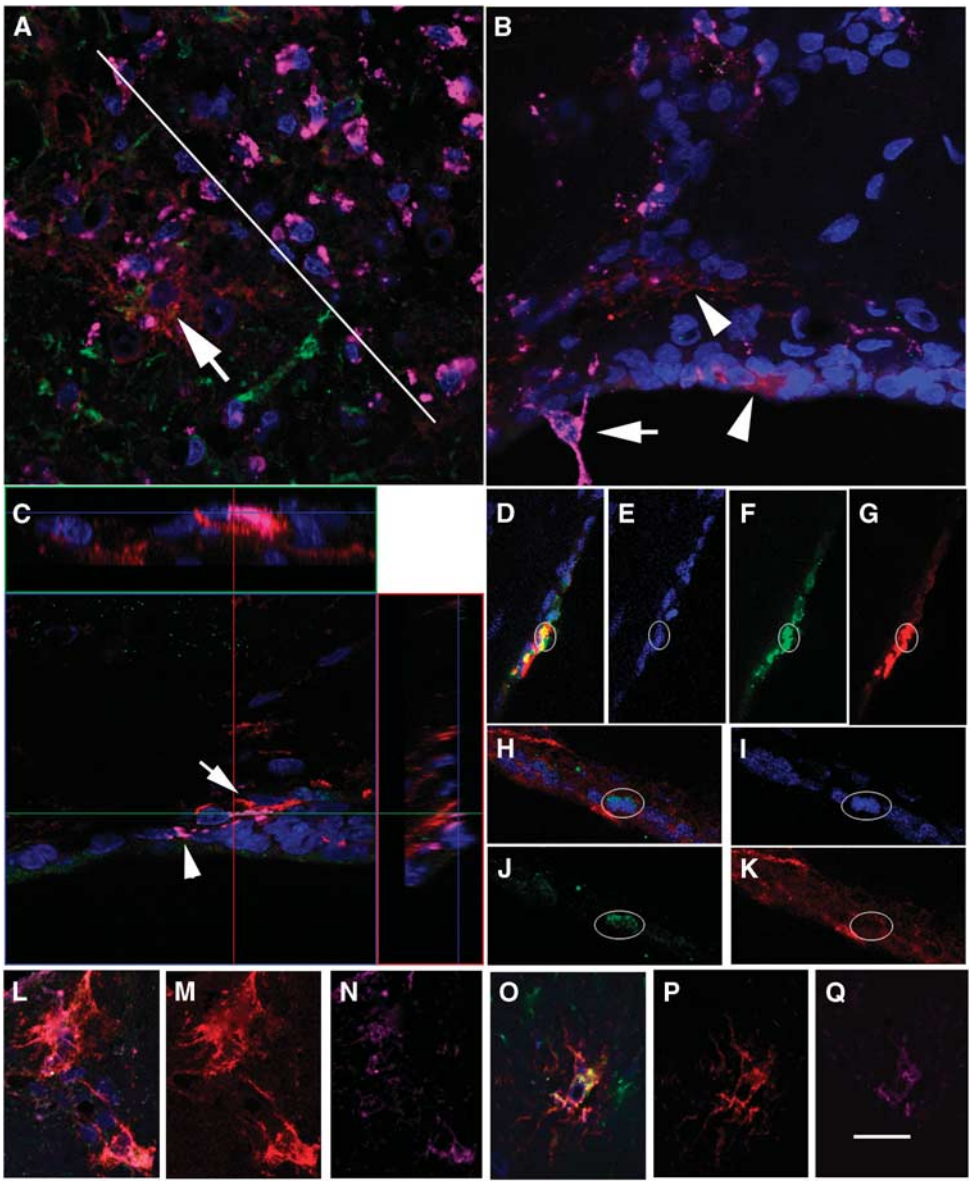

Figure 4 (**A**) At day 7, regions of the peri-infarct (below white line) and infarct (above white line) in Area X together with staining for αSMA (red), glial fibrillary acidic protein (GFAP) (green), and ED1 (pink). Within the peri-infarct there are less numbers of ED1-positive cells (pink), which are greater in number within the infarct (above the white line). A large αSMA + cell (arrow) and a GFAP + cell (green, αSMA−) are located close to the infarct. (**B**) ED1 + cells are clearly distinguishable from αSMA + cells (arrowheads). One ED1 + cell (arrow) protrudes into the ventricle. (**C**) Cells that express αSMA can be distinguished from those that are ED1 + using an orthogonal view. (**D**–**K**) Evidence of two cells within the subventricular zones (SVZ) (**D**–**G** and **H**–**K**) that appear to be αSMA + (red, **G**, **K**) and express Ki67 + (green, **F**, **J**) within the nucleus (DAPI, blue, **E**, **I**). The composite images for each example are shown in (**D**, **H**). (**L**–**N**) A cell located in Area A that coexpresses αSMA (**M**, red), feline leukemia virus C receptor 2 (FLVCR2) (**N**, pink) and shown as a composite (**L**; DAPI, blue). (**O**–**Q**) A cell located in Area X that coexpresses αSMA (**P**, red), FLVCR2 (**Q**, pink) and shown as a composite (**O**; DAPI, blue). These cells also express GFAP (green) in the composites but not shown in a separate panel. The calibration bar in (**Q**) equals 50 μm in (**D**–**G**), 40 μm in (**A**, **L**–**Q**), 25 μm in (**B**, **H**–**K**), and 20 μm in (**C**). SMA, smooth muscle actin.

Within the SVZ and its adjacent areas, ED1-positive cells could be distinguished from neighboring αSMA + cells using the orthogonal display facility of the LSM Image Browser software (Figure 4C). There appeared to be no crossreactivity of αSMA + cells with ED1 within the vicinity of the SVZ.

Evidence for the Coexpression of Ki67 and α-Smooth Muscle Actin in the Subventricular Zones

At day 7, the SVZ was investigated for cells that coexpressed αSMA with Ki67, a marker of cells that are not in the G_0-phase and therefore have recently

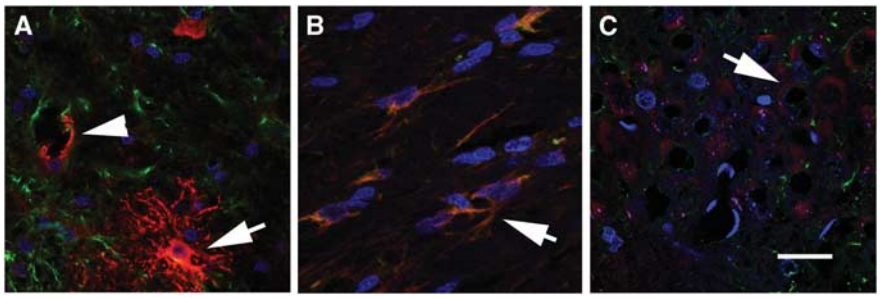

Figure 5 (**A**) At day 14, αSMA + cells (red) are shown that display Morphology 1 (arrow) while others are associated with vessels (arrowhead, Morphology 2) in Area X. These examples are negative for glial fibrillary acidic protein (GFAP) (green). (**B**) Many of the αSMA + cells (red channel, Morphology 2) are incorporated into vessel walls and are positive for NG2 (green channel) and thus appear orange in this panel. (**C**) αSMA + cells (red, low fluorescence intensity) are shown that are associated with lumen (arrows) but are GFAP-negative (green) and NG2-negative (pink). The calibration bar in (**C**) represents 25 μm in (**B**) and 40 μm in (**A**–**C**). SMA, smooth muscle actin.

proliferated. Although the antibody used here had been successfully tested in human cell lines in our laboratory, within the SVZ there were few Ki67 + cells in each rat tissue section. However, some cells were clearly Ki67 + and some associated with αSMA + staining (Figures 4D–G and 4H–K). These examples suggest that αSMA + cells are born within the SVZ.

α-Smooth Muscle Actin + Cell Populations in Area X at Day14

By day 14 (Area X), there was diminished evidence of αSMA + cells with Morphology 1 and more structures displayed Morphology 2 (Figures 1E and 1G and 5A and 5B). A majority of these cells were also positive for NG2 (Figure 5B), which is consistent with their identity as pericytes.

In this region, there are also examples of weaker fluorescence of αSMA + structures surrounding lumen (Figure 5C). These are GFAP-negative, NG2-negative (Figure 5C), and PDGFRβ-negative (data not shown).

Discussion

This manuscript describes the expression of αSMA by unique populations of cells at specific loci within the ipsilateral (compared with the contralateral) hemisphere, which alter in cell numbers with time after the induction of cerebral ischemia. These observations were predicated on the use of the anti-αSMA antibody that according to the distributors (DAKO) is identical to the anti-αsm-1 antibody characterized by Skalli *et al* (1986), which identifies rat and human αSMA in contrast to β- and γSMA.

In the CNS (central nervous system), two populations of αSMA + cells have been well documented namely, vascular smooth muscle cells that are normally integrated into the vessel wall of larger arterioles and arteries, and pericytes that normally form a close interaction with endothelial cells that line smaller blood vessels. A single report in 1991 by Lecain *et al* (1991) described αSMA + /GFAP + cells with morphology similar to some astrocytes that were found in the corpus callosum and fornix of normal C57B6 adult mice. Although the numbers of mice investigated in the study was unclear, it was noted that astrocytic processes were αSMA + but only in the sagittal plane, an unexpected result (Lecain *et al*, 1991). We found little evidence of αSMA + /GFAP + cells in the corpus callosum on the contralateral side in the SHR rat model (Figures 3C and 3F). As described here, large numbers of αSMA + /GFAP− (71%) and αSMA + /GFAP + (29%) were found in Areas A (corpus callosum) and Area B (Figure 3), 3 days after induction of ischemia. Pericytes precursors do express GFAP reflecting a partially differentiated phenotype (Dore-Duffy *et al*, 2011) and the multipotential nature of these precursors. There were also large numbers of GFAP + cells (αSMA−), particularly in Area B, which were presumably astrocytes (Figure 3H).

In summary of the data obtained by quantification, αSMA + cells (Morphology 1) were at maximum numbers at day 3 in Area A. In subsequent days there was a steady decline in Area A, which coincided with increasing numbers counted in Area X (day 7, Morphology 1; day 14, Morphology 2) consistent with incorporation of αSMA + cells into small vessels in the peri-infarct region between days 7 and 14. These observations would also be consistent with the migration of αSMA + (Morphology 1) cells into the peri-infarct from Area A up to day 7 and thereafter incorporation into small vessels by day 14. Alternatively, a mechanism and function for the sequential up and downregulation of αSMA by cells (Morphology 1) in Areas A and B and subsequently in Areas X and Y in the peri-infarct would require definition. A possible function might include the control of blood flow in capillary beds of the vascular system stemming from the MCA.

The migration hypothesis would imply a site(s) of origin. Clues to the possible origins of αSMA + cells

in Areas A and B were found using multilabeling and confocal microscopy as shown in Figures 3G and 3H, respectively. At day 3, αSMA+ cells were evident within and adjacent to a zone within the subventricular layer, consistent with proliferation from two regions of the SVZ and separate pathways of migration away through Areas A and B. In Figures 4D–K (day 7), there is evidence that αSMA+ cells within the SVZ also express levels of Ki67, a marker associated with recent cell-cycle activity (not expressed in the G_0-phase). However, in this region, there are extensive networks of capillaries and it is possible that αSMA+ precursors infiltrate the specific loci of Areas A, B, X and others for reasons that are not yet clear. The proposed migration of αSMA+ cells (Morphology 1) would clearly be an interesting phenomenon and would require further extensive experimentation in which potential αSMA+ cells born in the SVZ were labeled and identified subsequently in the Areas defined above at the appropriate time points.

While the proof of migration of αSMA+ cells with Morphology 1 requires further experimentation, the migration of various cell types has previously been demonstrated in response to injury or insult. The increased migration of NSPCs has been reported in several studies and these cells appear to originate from several loci as presented in the Introduction. Nakagomi *et al* (2011) have described NSPCs that arise from the leptomeninges in response to ischemia and there is evidence of a few αSMA+ cells (Morphology 1) close to those structures in the peri-infarct, perhaps implicating this site as a minor proliferation zone. Holmin *et al* (1997) described subependymal cells (nestin+) that were presumptive stem cells as well as committed precursors that migrate and differentiate into GFAP+ astrocytes in adult brain in response to brain injury (physical). The GFAP+ cells in Area B (day 3; Figure 3H) may represent such a population. Likewise, progenitor cells of the SVZ proliferate, migrated and differentiated into oligodendrocytes and astrocytes in response to demyelination injury in the corpus callosum (Nait-Oumesmar *et al*, 1999). The peak of migration was about 14 days after injury. Furthermore, labeled precursor cells that originated from the SVZ migrated into the corpus callosum and into the area of infarct with morphologies that suggested glial cells, in a mouse model of cerebral injury (Goings *et al*, 2004). Thus, the proliferation, migration, and differentiation of different lineages of the CNS in adult depend on the type of lesion. One established origin for a range of cell types appears to be the SVZ and the time for maximal response is 14 to 21 days.

Multilabeling and confocal microscopy can be useful to establish other markers expressed by cells and help confirm cell identity. Other than GFAP expression by a subpopulation at day 3 (discussed above), the αSMA+ cells (Morphology 1) were negative for nestin (marker of undifferentiated cells), negative for markers of mature pericytes when associated with vessels namely, desmin, PDGFRβ and NG2, and negative for a marker of microglia and macrophages ED1 (Figures 4A–C). However, the αSMA+ cells (Morphology 1) reported here did not express other markers except FLVCR2 (Figures 4N and 4Q), which was implicated as a marker of fetal pericytes (Thomas *et al*, 2010). Two antibodies against separate epitopes of FLVCR2 (including MAb 3D5; Figure 4) demonstrated αSMA-positive pericytes expressed FLVCR2. This transporter of heme (FLVCR2) was also found to be expressed by GFAP+ (αSMA−) astrocytes in this study (data not shown), which might suggest both cell types are responding to the local (stressed) microenvironment, in which heme metabolism might be an important outcome. We conclude that the αSMA+ cells with Morphology 1 represent a novel population that has not been previously described.

Large populations of ED1-positive cells were identified in the infarct (Figure 4A) and were presumably macrophages that had infiltrated from blood. Elsewhere αSMA-positive cells (Morphology 1) were clearly ED1-negative (Figures 4B and 4C) and therefore unlikely to be microglia (ED1-positive).

Increasingly, there were a large number of αSMA+ cells associated with vessels (Morphology 2: Figures 1E and 1G) and in the peri-infarct these were also NG2-positive consistent with their identity as pericytes (Figure 5B). At day 14, a further population of αSMA+ cells with reduced fluorescence intensity was observed under higher magnification in the peri-infarct region, Area X (Figure 5C).

Pericytes involved in angiogenesis in infarct tissue have previously been reported to originate from the circulation and are bone marrow derived (Rajantie *et al*, 2004; Kokovay *et al*, 2006; Lamagna and Bergers, 2006). It has also been proposed that these cells result from cell fusion (Piquer-Gil *et al*, 2009). However, it is possible that there are at least two populations of pericytes recruited into the damaged tissue, one that originates from the SVZ and migrates into the peri-infarct (as proposed in this manuscript), another from the blood that infiltrates the infarct core and originate from the bone marrow and possibly a third population that arises from the area of damaged cells.

Migration of precursors of pericytes has been described in the fetal developing brain. Neural crest cell progenitors are believed to disappear with closure of the neural tube, but niches persist in adult in the enteric and dorsal root ganglia, hair follicles, teeth and bone marrow. Thus, the possibility that the putative pericytes described here are born in restricted zones of the SVZ and migrate in response to brain damage raises the further possibility that these are NCC-like cells.

Immortalized precursors of murine pericytes with proliferative potential express PDGFRβ and NG2, but not αSMA (Dore-Duffy *et al*, 2011). With basic fibroblast growth factor immortalized pericytes form neurospheres and many cells appear to coexpress markers for pericytes (NG2), neurons (NF), astrocytes

(GFAP), and oligodendrocytes (O4), suggesting an immature phenotype (Dore-Duffy *et al*, 2011). We had observed αSMA + cells (putative pericytes) some of which also expressed GFAP, which might also be consistent with an immature phenotype of cells that go on to differentiate into astrocytes (αSMA−).

One important question that also arises from our study and the migration hypothesis is the nature of the signaling mechanism that might initiate proliferation and migration. Local factors in the hypoxic microenvironment of ischemia initiate complex cellular and molecular responses via transcriptional activation of genes in recruited precursor cells. Thus, hypoxia drives angiogenesis via local expression of hypoxia-inducible factors (HIF 1, 2, 3) and expression of vascular endothelial growth factors. Vascular endothelial growth factor isoforms fulfil different functions during angiogenesis including pericyte recruitment.

It is unlikely that these local factors induced by hypoxia in the peri-infarct could be directly responsible for initiating proliferation and migration of the αSMA + cells as proposed. It is possible that neurons that send axons along the corpus callosum, the proposed route of migration for the pericyte precursors to the peri-infarct, provide the stimulus for these events of pericyte proliferation and migration. Such stimuli might arise from the relatively slow mechanisms of retrograde transport that have been described for damaged neurons (Hendry *et al*, 1995; Johanson *et al*, 1995; Weible *et al*, 2004).

In summary, this manuscript provides evidence of a novel population of αSMA + cells, born in response to ischemia associated with the induction of stroke. It is hypothesized that these cells originate from neural crest precursors in the SVZ, migrate over several days along discrete pathways into the peri-infarct and are incorporated into vessels. Further research is aimed at demonstrating this hypothesis.

Disclosure/conflict of interest

The authors declare no conflict of interest.

References

Brasier G, Tikellis C, Xuereb L, Craigie J, Casley D, Kovacs CS, Fudge NJ, Kalnins R, Cooper ME, Wookey PJ (2004) Novel hexad repeats conserved in a putative transporter with restricted expression in cell types associated with growth, calcium exchange and homeostasis. *Exp Cell Res* 293:31–42

Dore-Duffy P (2008) Pericytes: pluripotent cells of the blood brain barrier. *Curr Pharm Des* 14:1581–93

Dore-Duffy P, Mehedi A, Wang X, Bradley M, Trotter R, Gow A (2011) Immortalized CNS pericytes are quiescent smooth muscle actin-negative and pluripotent. *Microvasc Res* 82:18–27

Duffy SP, Shing J, Saraon P, Berger LC, Eiden MV, Wilde A, Tailor CS (2010) The Fowler syndrome-associated protein FLVCR2 is an importer of heme. *Mol Cell Biol* 30:5318–24

Etchevers HC, Vincent C, Le Douarin NM, Couly GF (2001) The cephalic neural crest provides pericytes and smooth muscle cells to all blood vessels of the face and forebrain. *Development* 128:1059–68

Goings GE, Sahni V, Szele FG (2004) Migration patterns of subventricular zone cells in adult mice change after cerebral cortex injury. *Brain Res* 996:213–26

Hendry IA, Johanson SO, Heydon K (1995) Retrograde axonal transport of the alpha subunit of the GTP-binding protein Gz to the nucleus of sensory neurons. *Brain Res* 700:157–63

Holmin S, Almqvist P, Lendahl U, Mathiesen T (1997) Adult nestin-expressing subependymal cells differentiate to astrocytes in response to brain injury. *Eur J Neurosci* 9:65–75

Jeynes B (1985) Reactions of granular pericytes in a rabbit cerebrovascular ischemia model. *Stroke* 16:121–5

Jin K, Minami M, Lan JQ, Mao XO, Batteur S, Simon RP, Greenberg DA (2001) Neurogenesis in dentate subgranular zone and rostral subventricular zone after focal cerebral ischemia in the rat. *Proc Natl Acad Sci USA* 98:4710–5

Johanson SO, Crouch MF, Hendry IA (1995) Retrograde axonal transport of signal transduction proteins in rat sciatic nerve. *Brain Res* 690:55–63

Kojima T, Hirota Y, Ema M, Takahashi S, Miyoshi I, Okano H, Sawamoto K (2010) Subventricular zone-derived neural progenitor cells migrate along a blood vessel scaffold toward the post-stroke striatum. *Stem Cells* 28:545–54

Kokovay E, Li L, Cunningham LA (2006) Angiogenic recruitment of pericytes from bone marrow after stroke. *J Cereb Blood Flow Metab* 26:545–55

Kronenberg G, Wang LP, Synowitz M, Gertz K, Katchanov J, Glass R, Harms C, Kempermann G, Kettenmann H, Endres M (2005) Nestin-expressing cells divide and adopt a complex electrophysiologic phenotype after transient brain ischemia. *J Cereb Blood Flow Metab* 25:1613–24

Lamagna C, Bergers G (2006) The bone marrow constitutes a reservoir of pericyte progenitors. *J Leukoc Biol* 80: 677–81

Lecain E, Alliot F, Laine MC, Calas B, Pessac B (1991) Alpha isoform of smooth muscle actin is expressed in astrocytes *in vitro* and *in vivo*. *J Neurosci Res* 28:601–6

Lindahl P, Johansson BR, Leveen P, Betsholtz C (1997) Pericyte loss and microaneurysm formation in PDGF-B-deficient mice. *Science* 277:242–5

Nait-Oumesmar B, Decker L, Lachapelle F, Avellana-Adalid V, Bachelin C, Van Evercooren AB (1999) Progenitor cells of the adult mouse subventricular zone proliferate, migrate and differentiate into oligodendrocytes after demyelination. *Eur J Neurosci* 11:4357–66

Nakagomi T, Molnar Z, Nakano-Doi A, Taguchi A, Saino O, Kubo S, Clausen M, Yoshikawa H, Nakagomi N, Matsuyama T (2011) Ischemia-induced neural stem/progenitor cells in the pia mater following cortical infarction. *Stem Cells Dev* 20:2037–51

Nakagomi T, Taguchi A, Fujimori Y, Saino O, Nakano-Doi A, Kubo S, Gotoh A, Soma T, Yoshikawa H, Nishizaki T, Nakagomi N, Stern DM, Matsuyama T (2009) Isolation and characterization of neural stem/progenitor cells from post-stroke cerebral cortex in mice. *Eur J Neurosci* 29:1842–52

Ohira K, Furuta T, Hioki H, Nakamura KC, Kuramoto E, Tanaka Y, Funatsu N, Shimizu K, Oishi T, Hayashi M,

Miyakawa T, Kaneko T, Nakamura S (2010) Ischemia-induced neurogenesis of neocortical layer 1 progenitor cells. *Nat Neurosci* 13:173–9

Pardanaud L, Yassine F, Dieterlen-Lievre F (1989) Relationship between vasculogenesis, angiogenesis and haemopoiesis during avian ontogeny. *Development* 105:473–85

Parent JM, Vexler ZS, Gong C, Derugin N, Ferriero DM (2002) Rat forebrain neurogenesis and striatal neuron replacement after focal stroke. *Ann Neurol* 52:802–13

Petullo D, Masonic K, Lincoln C, Wibberley L, Teliska M, Yao DL (1999) Model development and behavioral assessment of focal cerebral ischemia in rats. *Life Sci* 64:1099–108

Piquer-Gil M, Garcia-Verdugo JM, Zipancic I, Sanchez MJ, Alvarez-Dolado M (2009) Cell fusion contributes to pericyte formation after stroke. *J Cereb Blood Flow Metab* 29:480–5

Rajantie I, Ilmonen M, Alminaite A, Ozerdem U, Alitalo K, Salven P (2004) Adult bone marrow-derived cells recruited during angiogenesis comprise precursors for periendothelial vascular mural cells. *Blood* 104:2084–6

Renner O, Tsimpas A, Kostin S, Valable S, Petit E, Schaper W, Marti HH (2003) Time- and cell type-specific induction of platelet-derived growth factor receptor-beta during cerebral ischemia. *Brain Res Mol Brain Res* 113:44–51

Rewell SS, Fernandez JA, Cox SF, Spratt NJ, Hogan L, Aleksoska E, van Raay L, Liberatore GT, Batchelor PE, Howells DW (2010) Inducing stroke in aged, hypertensive, diabetic rats. *J Cereb Blood Flow Metab* 30:729–33

Shimada IS, Peterson BM, Spees JL (2010) Isolation of locally derived stem/progenitor cells from the peri-infarct area that do not migrate from the lateral ventricle after cortical stroke. *Stroke* 41:e552–60

Sieczkiewicz GJ, Herman IM (2003) TGF-beta 1 signaling controls retinal pericyte contractile protein expression. *Microvasc Res* 66:190–6

Skalli O, Ropraz P, Trzeciak A, Benzonana G, Gillessen D, Gabbiani G (1986) A monoclonal antibody against alpha-smooth muscle actin: a new probe for smooth muscle differentiation. *J Cell Biol* 103:2787–96

Spratt NJ, Fernandez J, Chen M, Rewell S, Cox S, van Raay L, Hogan L, Howells DW (2006) Modification of the method of thread manufacture improves stroke induction rate and reduces mortality after thread-occlusion of the middle cerebral artery in young or aged rats. *J Neurosci Methods* 155:285–90

Takahashi A, Park HK, Melgar MA, Alcocer L, Pinto J, Lenzi T, Diaz FG, Rafols JA (1997) Cerebral cortex blood flow and vascular smooth muscle contractility in a rat model of ischemia: a correlative laser Doppler flowmetric and scanning electron microscopic study. *Acta Neuropathol* 93:354–68

Tavazoie M, Van der Veken L, Silva-Vargas V, Louissaint M, Colonna L, Zaidi B, Garcia-Verdugo JM, Doetsch F (2008) A specialized vascular niche for adult neural stem cells. *Cell Stem Cell* 3:279–88

Thomas S, Encha-Razavi F, Devisme L, Etchevers H, Bessieres-Grattagliano B, Goudefroye G, Elkhartoufi N, Pateau E, Ichkou A, Bonniere M, Marcorelle P, Parent P, Manouvrier S, Holder M, Laquerriere A, Loeuillet L, Roume J, Martinovic J, Mougou-Zerelli S, Gonzales M, Meyer V, Wessner M, Feysot CB, Nitschke P, Leticee N, Munnich A, Lyonnet S, Wookey P, Gyapay G, Foliguet B, Vekemans M, Attie-Bitach T (2010) High-throughput sequencing of a 4.1 Mb linkage interval reveals FLVCR2 deletions and mutations in lethal cerebral vasculopathy. *Hum Mutat* 31:1134–41

Verbeek MM, Otte-Holler I, Wesseling P, Ruiter DJ, de Waal RM (1994) Induction of alpha-smooth muscle actin expression in cultured human brain pericytes by transforming growth factor-beta 1. *Am J Pathol* 144:372–82

Weible 2nd MW, Ozsarac N, Grimes ML, Hendry IA (2004) Comparison of nerve terminal events *in vivo* effecting retrograde transport of vesicles containing neurotrophins or synaptic vesicle components. *J Neurosci Res* 75:771–81

Yemisci M, Gursoy-Ozdemir Y, Vural A, Can A, Topalkara K, Dalkara T (2009) Pericyte contraction induced by oxidative-nitrative stress impairs capillary reflow despite successful opening of an occluded cerebral artery. *Nat Med* 15:1031–7

Zhang RL, Zhang ZG, Zhang L, Chopp M (2001) Proliferation and differentiation of progenitor cells in the cortex and the subventricular zone in the adult rat after focal cerebral ischemia. *Neuroscience* 105:33–41